Appendix

In A, we provide the details for assessing the persistence of a population with an integrodifference model and we discuss the effect of the harvesting function on population persistence. In B, we provide the details for assessing population persistence with separable dispersal kernels. In C and D, we derive expressions for the critical harvesting rate and rate of environmental shift for Gaussian and sinuosoidal dispersal kernels. In E, we derive approximate expressions for these critical rates. In F, we parameterize our model for black rockfish (*Sebastes melanops*) in the California Current and demonstrate that results for parameters are qualitatively similar to results presented in the main text. In G, we provide details on differences between small and large MPA simulations.

A) Determining stability

Let $n_t(x)$ be the number of adults at position x at time t, let $k(x)$ be a dispersal kernel describing the probability of a larva traveling a distance x. Let $f(n)$ be the recruitment function describing the number of offspring that settle and survive in juvenile population of size n, let R_0 be the intrinsic growth rate of the population, and let $g(n)$ be the harvesting function describing the number of adults harvested from a population of size n. In the absence of harvesting, the integrodifference model describing the population over time is given by

$$n_{t+1}(x) = \int_{-L/2+ct}^{L/2+ct} k(x-y) R_0 f\left(n_t(y)\right) dy \tag{A.1}$$

as described in (Zhou and Kot 2011). With the addition of harvesting, the model becomes

$$n_{t+1}(x) = \int_{-L/2+ct}^{L/2+ct} k(x-y) R_0 g\left(f\left(n_t(y)\right)\right) dy. \tag{A.2}$$

In evaluating persistence, we apply the methods of Zhou and Kot (2011) to the new model, Equation 2. A traveling pulse is a solution such that population size relative to location within the patch (rather than absolute position) is constant over time, i.e.,

$$n^*(\bar{x}_t) \equiv n^*(x-ct) = n_t(x)$$

where $\bar{x}_t \equiv x - ct$ gives position relative to the patch.

The integrodifference Eq. 2 gives us an expression for n^*:

$$n^*(\bar{x}_{t+1}) = n_{t+1}(x)$$

$$n^*(\bar{x}_{t+1}) = \int_{-L/2+ct}^{L/2+ct} k(x-y) R_0 g\left(f\left(n_t(y)\right)\right) dy$$

$$n^*(\bar{x}_{t+1}) = \int_{-L/2+ct}^{L/2+ct} k(x-\bar{y}_t-ct) R_0 g\left(f\left(n^*(\bar{y}_t)\right)\right) dy$$

$$n^*(\bar{x}_{t+1}) = \int_{-L/2+ct}^{L/2+ct} k(\bar{x}_t-\bar{y}_t) R_0 g\left(f\left(n^*(\bar{y}_t)\right)\right) dy$$

$$\Rightarrow n^*(\bar{x}_t - c) = \int_{-L/2+ct}^{L/2+ct} k(\bar{x}_t-\bar{y}_t) R_0 g\left(f\left(n^*(\bar{y}_t)\right)\right) dy$$

$$\Rightarrow n^*(\bar{x}_t) = \int_{-L/2}^{L/2} k(\bar{x}_t+c-\bar{y}_t) R_0 g\left(f\left(n^*(\bar{y}_t)\right)\right) d\bar{y}_t \tag{A.3}$$

As long as $f(0) = 0$, there is a trivial solution to this problem where $n^*(\bar{x}) \equiv 0$ for all $\bar{x}$, i.e., there is a trivial traveling pulse with no adults in it. If the trivial traveling pulse is unstable, even very small populations will persist or grow and avoid crashing back to the trivial pulse. To evaluate the stability of a traveling pulse, we introduce a small perturbation to the traveling pulse $n^*(\bar{x})$ and see if this perturbation grows or shrinks over time:

$$n_t(x) = n^*(\bar{x}_t) + \xi_t(x)$$

$$\Rightarrow \xi_{t+1}(x) = n_{t+1}(x) - n^*(\bar{x}_{t+1})$$

$$\xi_{t+1}(x) = n_{t+1}(x) - n^*(\bar{x}_t - c)$$

$$\xi_{t+1}(x) = \int_{-L/2+ct}^{L/2+ct} k(x-y) R_0 g\left(f\left(n_t(y)\right)\right) dy - \int_{-L/2}^{L/2} k(\bar{x}_t - \bar{y}_t) R_0 g\left(f\left(n^*(\bar{y}_t)\right)\right) d\bar{y}_t \text{ using Eq.3}$$

$$\xi_{t+1}(x) = \int_{-L/2+ct}^{L/2+ct} k(x-y) R_0 g\left(f\left(n_t(y)\right)\right) dy - \int_{-L/2+ct}^{L/2+ct} k\left(x-ct-(y-ct)\right) R_0 g\left(f\left(n^*(\bar{y}_t)\right)\right) d\bar{y}_t$$

$$\xi_{t+1}(x) = \int_{-L/2+ct}^{L/2+ct} k(x-y) R_0 g\left(f\left(n_t(y)\right)\right) dy - \int_{-L/2+ct}^{L/2+ct} k(x-y) R_0 g\left(f\left(n^*(\bar{y}_t)\right)\right) d\bar{y}_t$$

$$\xi_{t+1}(x) = \int_{-L/2+ct}^{L/2+ct} k(x-y)\left(R_0 g\left(f\left(n_t(y)\right)\right) - R_0 g\left(f\left(n^*(\bar{y}_t)\right)\right)\right) dy$$

$$\xi_{t+1}(x) = \int_{-L/2+ct}^{L/2+ct} k(x-y) R_0 \left(g\left(f\left(n_t(y)\right)\right) - g\left(f\left(n^*(\bar{y}_t)\right)\right)\right) dy$$

$$\Rightarrow \xi_{t+1}(x) = \int_{-L/2+ct}^{L/2+ct} k(x-y) R_0 g'\left(f\left(n^*(\bar{y})\right)\right) f'\left(n^*(\bar{y})\right)\left(n_t(y) - n^*(\bar{y}_t)\right) dy$$

by linearizing around the traveling pulse

$$\Rightarrow \xi_{t+1}(x) = \int_{-L/2+ct}^{L/2+ct} k(x-y) R_0 g'\left(f\left(n^*(\bar{y})\right)\right) f'\left(n^*(\bar{y})\right) \xi_t(y)\, dy$$

$$\Rightarrow \xi_{t+1}(x) = \int_{-L/2+ct}^{L/2+ct} k(x-y) R_0 g'(0) f'(0) \xi_t(y)\, dy \qquad \text{(A.4)}$$

if $n^*(\bar{x}) = 0$ and $f(0) = 0$.

If we assume $\xi_t(x) = \lambda^t u(x-ct)$ for some $\lambda \in \mathbb{R}$ and $u:[-L/2, L/2] \to \mathbb{R}$, then the perturbation grows in time if and only if $\lambda > 1$. Using Eq. 4, we can rewrite $\xi_{t+1}(x)$,

$$\lambda u(x-ct-c) = R_0 g'(0) f'(0) \int_{-L/2+ct}^{L/2+ct} k(x-y) u(y-ct)\, dy$$

$$\Rightarrow \lambda u(\bar{x}) = R_0 g'(0) f'(0) \int_{-L/2}^{L/2} k(\bar{x}+c-\bar{y}) u(\bar{y})\, dy$$

define the integral operator,

$$\psi_f(u)(x) = R_0 g'(0) f'(0) \int_{-L/2}^{L/2} k(x+c-y) u(y)\, dy.$$

Then the perturbation to the traveling pulse will satisfy

$$\psi_f(u)(x) = \lambda u(x) \qquad \text{(A.5)}$$

λ and u are thus an eigenvalue and eigenfunction of the functional operator Ψ_f. The trivial traveling pulse is unstable when the dominant eigenvalue of Ψ_f is greater than 1.

The biomass in the equilibrium traveling wave depends on the specific functional forms of the harvesting function $g(n)$ and the recruitment function $f(n)$. However, the persistence of the population only depends on R_0, $g'(0)$ and $f'(0)$. In this paper, we only considered a proportional harvesting function, i.e. the amount of adults harvested obeyed $g(n) = (1-h)n$. For this function, $g'(0) = 1 - h$. For the recruitment function we considered, $f'(0) = 1$.

B) Separable dispersal kernels

It is not immediately obvious that the operator Ψ will have any eigenfunctions. However, Jentzsch's theorem guarantees that there is an eigenfunction u, provided that the kernel k satisfies some properties (Zhou and Kot 2011). Finding the eigenfunctions and eigenvalues is in general a hard problem to solve. It becomes easier if the kernel k is separable, i.e., there are functions a_n, b_n such that $k(x-y) = \sum_{n=1}^{\infty} a_n(x) b_n(y)$. In that case, Eq. 5 becomes

$$\lambda u(x) = R_0 g'(0) f'(0) \sum_{n=1}^{\infty} \left(a_n(x) \int_{-L/2}^{L/2} b_n(y-c) u(y) dy \right)$$

$$\Rightarrow \lambda \int_{-L/2}^{L/2} b_k(x-c) u(x) dx = R_0 g'(0) f'(0) \sum_{n=1}^{\infty} \left(\int_{-L/2}^{L/2} b_n(x-c) u(x) dx \right) \left(\int_{-L/2}^{L/2} a_n(y) b_k(y-c) dy \right)$$

for any k

$$\Rightarrow \lambda d_k = R_0 g'(0) f'(0) \sum_{n=1}^{\infty} A_{nk} d_n \tag{A.6}$$

where

$$A_{nk} = \int_{-L/2}^{L/2} a_n(x) b_k(x-c) dx \text{ and } d_k = \int_{-L/2}^{L/2} b_k(x-c) u(x) dx$$

Finding the eigenvalues of Eq. 5 then reduces to finding the eigenvalues of the matrix comprised of entires $(A_{nk})_{n,k=1}^{\infty}$.

To find the equilibrium biomass, we rewrite Eq. 3 using the separable kernel as in (Latore et al. 1998):

$$n^*(x) = \int_{-L/2}^{L/2} k(x+c-y) R_0 g\left(f\left(n^*(y)\right)\right) dy$$

$$n^*(x) = \int_{-L/2}^{L/2} \left(\sum_{n=1}^{\infty} a_n(x) b_n(y-c) \right) R_0 g\left(f\left(n^*(y)\right)\right) dy$$

$$n^*(x) = \sum_{n=1}^{\infty} a_n(x) \int_{-L/2}^{L/2} b_n(y-c) R_0 g\left(f\left(n^*(y)\right)\right) dy$$

If we define $m_n = \int_{-L/2}^{L/2} b_n(y-c) R_0 g\left(f\left(n^*(y)\right)\right) dy$ then we find that

$$n^*(x) = \sum_{n=1}^{\infty} m_n a_n(x) \text{ and}$$

$$m_n = \int_{-L/2}^{L/2} b_n(y-c) R_0 g\left(f\left(\sum_{n=1}^{\infty} m_n a_n(y) \right) \right) dy \qquad \text{(A.7)}$$

Eq 7. allows us to find the m_n numerically and we then find the total equilibrium biomass by integrating $n^*(x)$ over space.

C) Gaussian dispersal kernel

The Gaussian dispersal kernel is given by

$$k(x-y)=\frac{1}{2\sqrt{D\pi}}e^{\frac{-(x-y)^2}{4D}},$$

where D is one half the variance of the kernel. This is a separable kernel with

$a_n(x)=b_n(x)=\frac{1}{\sqrt{2n!\sqrt{D\pi}}}e^{-x^2/4D}\left(\frac{x}{\sqrt{2D}}\right)^n$ (Latore et al. 1998).

As a first approximation to k we ignore all but the 0^{th} terms for a_n and b_n so that Eq. 6 becomes

$$\lambda d_0(c)=R_0(1-h)A_{00}(c)d_0(c)$$

$$\Rightarrow \lambda = R_0(1-h)A_{00}(c)$$

$$\text{where } A_{00}(c)=2\sqrt{2}\exp\left(\frac{-c^2}{8D}\right)\left[erf\left(\frac{L-c}{2\sqrt{2D}}\right)-erf\left(\frac{-L-c}{2\sqrt{2D}}\right)\right]$$

where *erf* is the error function. The critical rate of environmental shift c^* and the critical harvesting rate h^* are those values of c and h, respectively, that make $\lambda = 1$.

D) Sinusoidal dispersal kernel

The sinusoidal dispersal kernel is given by

$$k(x-y)=\begin{cases}\frac{w}{2}\cos\left(w(x-y)\right) & , \quad |x-y|\le\frac{\pi}{2w}\\ 0 & , \quad |x-y|>\frac{\pi}{2w}\end{cases}$$

where L is the length of the patch and we assume $\frac{\pi}{2w}>L, c<\frac{\pi}{2w}-L$.

In this case, $k(x-y)=\frac{w}{2}\cos(wx)\cos(w(y-c))+\frac{w}{2}\sin(wx)\sin(w(y-c))$ so that A_{ij} and d_i can be found for $i, j = 1, 2$ and Eq. 6 reduces to

$$\lambda^2-\left(\frac{R_0(1-h)wL}{2}\cos(wc)\right)\lambda+\frac{R_0^2(1-h)^2}{16}\left(w^2L^2-\sin^2(wL)\right)=0.$$

If we solve for λ,we find

$$\lambda=(1-h)R_0\left[\frac{wL\cos(wc)}{4}+\frac{1}{4}\sqrt{\sin^2(wL)-w^2L^2\sin^2(wc)}\right].$$

Zhou and Kot (2011) solve for the critical speed, c^*, at which the population will be driven extinct:

$$c^*=c^*(R_0)=\frac{1}{w}\cos^{-1}\left[\frac{16+R_0^2(1-h)^2\left(w^2L^2-\sin^2(wL)\right)}{8R_0(1-h)wL}\right].$$

In our model, we can additionally solve for the critical harvesting rate, h^* at which the population will be driven extinct:

$$h^*=1-\frac{1}{R_0}\cdot\frac{4wL}{w^2L^2-\sin^2(wL)}\left[\cos(wc)-\sqrt{\cos^2(wc)-1+\frac{\sin^2(wL)}{w^2L^2}}\right]$$

E) Approximate critical harvesting proportions

We will use the following Taylor series to make approximations of the critical harvesting proportions under the two dispersal kernels:

$$\cos(x)=1-\frac{x^2}{2}$$

$$\cos^2(x) = 1 - x^2$$

$$\sin^2(x) = x^2 - \frac{x^4}{3}$$

$$erf(x) = \frac{2}{\sqrt{\pi}}\left(x - \frac{x^3}{3}\right)$$

$$\exp(x) = 1 + x + \frac{x^2}{2}$$

For the Gaussian kernel we found

$$h^* = 1 - \frac{2\sqrt{2}\exp\left(\frac{c^2}{8D}\right)}{R_0\left[erf\left(\frac{L-c}{2\sqrt{2D}}\right) - erf\left(\frac{-L-c}{2\sqrt{2D}}\right)\right]} \tag{A.8}$$

Using the Taylor series and the fact that $D = \frac{\sigma^2}{2}$ where σ^2 is the variance of the exponential kernel,

$$h^* \sim 1 - \frac{\sqrt{2\pi}\left(1 + \frac{c^2}{8D} + \frac{c^4}{128D^2}\right)}{R_0\sqrt{\pi}\left[\frac{L-c}{2\sqrt{2D}} - \frac{(L-c)^3}{3(2\sqrt{2D})^3} - \frac{-L-c}{2\sqrt{2D}} + \frac{(-L-c)^3}{3\left(2\sqrt{2D}\right)^3}\right]}$$

$$h^* = 1 - \frac{1}{R_0}\cdot\frac{3\sqrt{2\pi}}{8L}\frac{\left(32\sigma^4 + 8c^2\sigma^2 + c^4\right)}{\sigma\left(12\sigma^2 - \left(L^2 + 3c^2\right)\right)}$$

For the sinusoidal kernel we found

$$h^* = 1 - \frac{1}{R_0} \cdot \frac{4wL}{w^2L^2 - \sin^2(wL)} \left[\cos(wc) - \sqrt{\cos^2(wc) - 1 + \frac{\sin^2(wL)}{w^2L^2}} \right] \tag{A.9}$$

Using the Taylor series and the fact that $w = \frac{\sqrt{\frac{\pi^2}{4} - 2}}{\sigma}$ where σ^2 is the variance of the sinusoidal kernel,

$$h^* \sim 1 - \frac{1}{R_0} \cdot \frac{12wL}{w^4L^4} \left[1 - \frac{w^2c^2}{2} - \sqrt{1 - w^2c^2 - \frac{w^2L^2}{3}} \right]$$

$$h^* = 1 - \frac{1}{R_0} \cdot \frac{4\sqrt{3}}{L^3(\pi^2 - 8)^{3/2}} \cdot \sigma \left[8\sqrt{3}\sigma^2 - (\pi^2 - 8)\sqrt{3}c^2 - 4\sigma\sqrt{12\sigma^2 - (\pi^2 - 8)(3c^2 + L^2)} \right]$$

In the case of both kernels, the critical harvesting proportion can be approximated by a function that looks like

$$h^* \sim 1 - \frac{1}{R_0} \cdot p(L)\, q\left(\sigma^2, c^2, L^2 + 3c^2\right) \tag{A.10}$$

where *p(L)* is a decreasing function of the length of the viable patch *L*.

F) California Current black rockfish parameterization

We parameterize our model for black rockfish (*Sebastes melanops*) in the California Current, with MPAs of spacing and width qualitatively similar to those in the Marine Life Projection Act (MLPA), and with a maximum climate velocity equal to that observed empirically. The parameters and references are provided in Table A1.

Our results with this parameterization are qualitatively similar to the results presented in the main text. In particular, we find the same negative relationship between critical harvesting rate h^* and the climate velocity c (Fig. A1) and an essentially additive interaction between the effects of the two stressors on biomass (Fig. A2). Additionally, our black rockfish parameterization has the same counterintuitive result that MPAs from which effort is displaced (rather than eliminated) can be worse than no MPA at all (compare Fig. A4A and A4D).

G) Protected area fluctuations

After the simulations come to equilibrium, the fluctuations in total biomass per generation fluctuate more in reserves that are larger and spaced farther apart than simulations in which the reserves that are smaller and more closely spaced (Fig. A3). The large reserves have a slightly larger average population, however large reserves here can induce fluctuations of biomass even in deterministic simulations. Thus we expect if reproduction was stochastic, large reserves spaced far apart would be more likely to result in extinction of the population than more closely spaced, smaller reserves. We find the same effect regardless of whether or not effort remains constant or is removed from the system.

TABLE A1. Rockfish parameters.

Parameter	Value	Source
$\langle d \rangle$	73 km	White et al. (2010)
R_0	2.86	White et al. (2010), equivalent to 1/(CRT)
h	0–100%	
L	1000 km	Froese (2014)
c	0–200 km/decade	Burrows et al. (2011)
Generation time	7 yr	Love (2011)
MPA width	20 km	Gaines et al. (2010)
Space between MPAs	76 km	Gaines et al. (2010)

LITERATURE CITED

Burrows, M. T., et al. 2011. The pace of shifting climate in marine and terrestrial ecosystems. Science 334:652–655.

Froese, R. 2014. FishBase. http://www.fishbase.org/summary/Sebastes-melanops.html

Gaines, S. D., S. E. Lester, K. Grorud-Colvert, C. Costello, and R. Pollnac. 2010. Evolving science of marine reserves: new developments and emerging research frontiers. Proceedings of the National Academy of Sciences 107: 8251–8255.

Latore, J., P. Gould, and A. M. Mortimer. 1998. Spatial dynamics and critical patch size of annual plant populations. Journal of Theoretical Biology 190:277–285.

Love, M. 2011. Certainly more than you want to know about the fishes of the Pacific Coast. Really Big Press, Santa Barbara, California, USA.

White, J. W., L. W. Botsford, E. A. Moffitt, and D. T. Fischer. 2010. Decision analysis for designing marine protected areas for multiple species with uncertain fishery status. Ecolological Applications 20:1523–1541.

Zhou, Y., and M. Kot. 2011. Discrete-time growth-dispersal models with shifting species ranges. Theoretical Ecology 4:13–25.

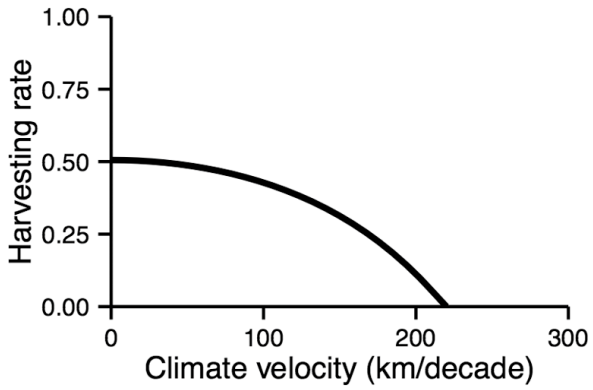

FIG. A1. The line indicates the critical harvesting rate as a function of climate velocity on the x-axis. These results are from an approximated Gaussian dispersal kernel parameterized for black rockfish.

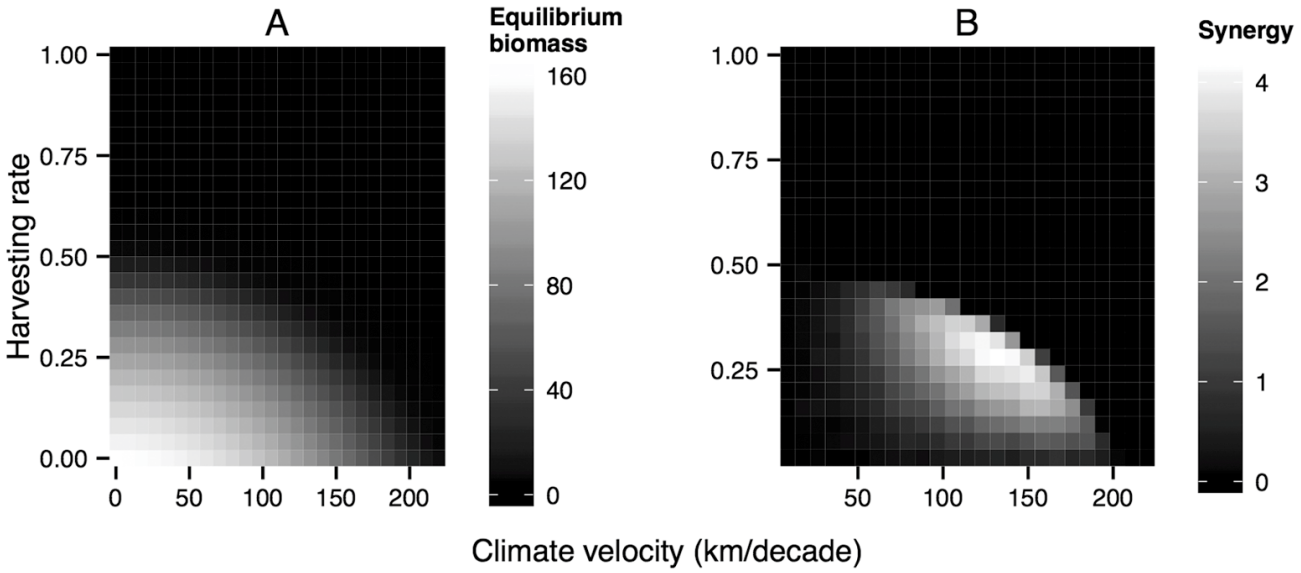

FIG. A2. (A) The equilibrium biomass of a black rockfish population as a function of the climate velocity on the x-axis and the harvesting rate on the *y*-axis. (B) Interaction between the two stressors as a function of climate velocity and harvesting rate. The heat map indicates the interaction measure *S*, as defined in Eq. 10, i.e., the loss in biomass in the doubly stressed population in excess of the sum of the losses caused by each stressor individually. *S* of zero indicates additive interaction of the stressors. The excess loss is small in comparison to the total biomass. These results are from an approximated Gaussian dispersal kernel parameterized for black rockfish.

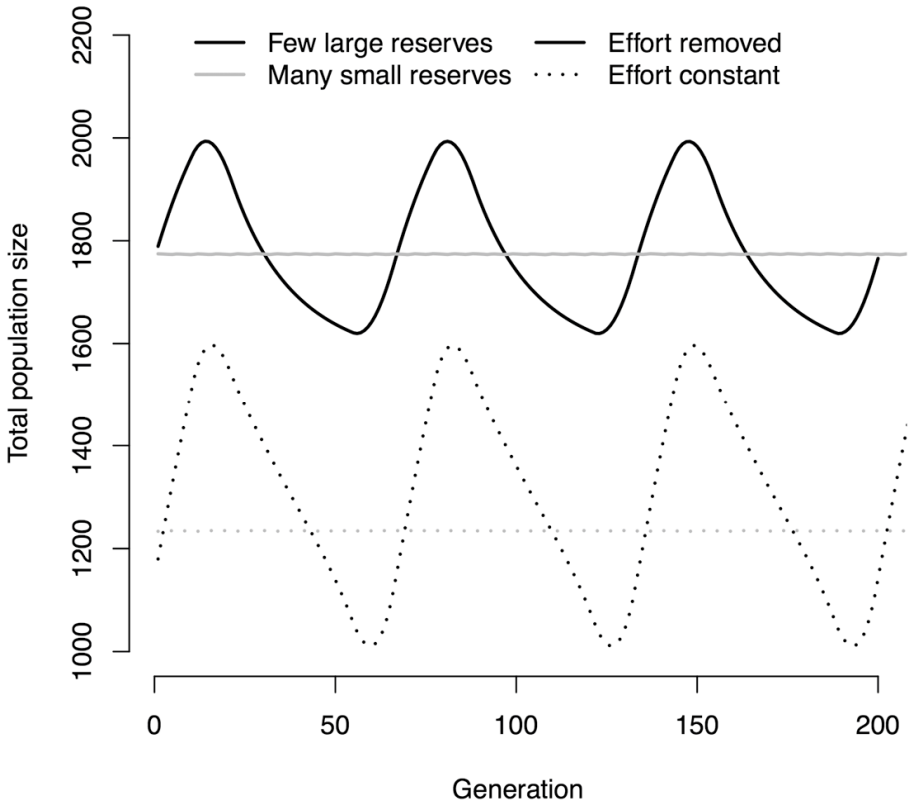

FIG. A3. Fluctuations in biomass caused by MPAs. We show biomass as a function of the number of generations for both many small and few large reserves and both removed harvesting pressure and constant harvesting pressure (i.e., reallocation). The fluctuations in biomass with many small reserves are small enough that the biomass appears nearly constant. While the biomass has a larger maximum with few large reserves, the fluctuations are much greater in magnitude. These results are from simulations with a Laplacian dispersal kernel with $c = 0.1$ and $h = 0.02$.

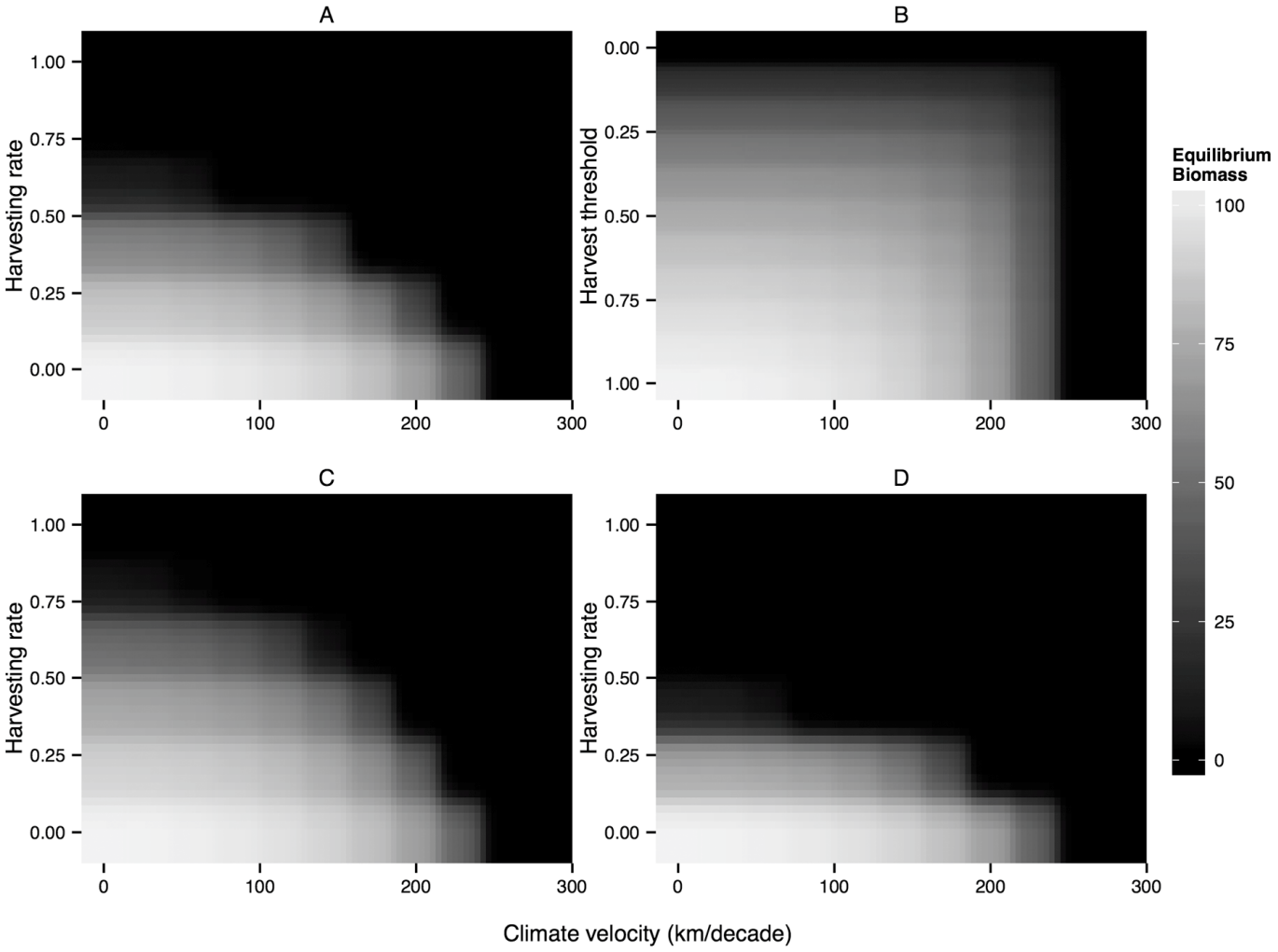

FIG. A4. The equilibrium biomass of the population as a function of the climate velocity on the *x*-axis and the harvesting rate on the *y*-axis under alternative management strategies. (A) The equilibrium biomass for simulations with constant harvest rates. (B) Equilibrium biomass for simulations with threshold management. For threshold management, we set a threshold density below which no fishing is allowed. The threshold ranges between zero (no fishing allowed) and one (all fish taken), with intermediate density thresholds determined as fractions of the maximum population density observed at a given time step before harvesting. We show this on the *y*-axis. (C) Equilibrium biomass for simulations with protected areas where harvesting pressure outside reserves is unchanged (i.e., harvest effort inside reserves is eliminated). (D) Equilibrium biomass

for simulations with protected areas in which harvesting pressure is reallocated outside reserves. These results are from simulations with a Laplacian dispersal kernel parameterized for black rockfish.